Restraining Expansion of the Peak Envelope in H/D Exchange−MS and Its Application in Detecting Perturbations of Protein Structure/Dynamics

ARTICLE *in* ANALYTICAL CHEMISTRY · SEPTEMBER 2008

Impact Factor: 5.64 · DOI: 10.1021/ac800897q · Source: PubMed

3 AUTHORS:

Gordon W Slysz
Cadwell Laboratories
31 PUBLICATIONS **627** CITATIONS
SEE PROFILE

Andrew John Percy
University of Victoria
33 PUBLICATIONS **570** CITATIONS
SEE PROFILE

David C Schriemer
The University of Calgary
92 PUBLICATIONS **2,391** CITATIONS
SEE PROFILE

Anal. Chem. **2008,** *80,* 7004–7011

Restraining Expansion of the Peak Envelope in H/D Exchange-MS and Its Application in Detecting Perturbations of Protein Structure/Dynamics

Gordon W. Slysz, Andrew J. Percy, and David C. Schriemer*

Department of Biochemistry and Molecular Biology, University of Calgary, Calgary, Alberta T2N 4N1, Canada

Hydrogen/deuterium exchange (H/DX) mass spectrometry (MS) is increasingly applied to problems in protein structural biology in order to map protein dynamics and identify sites of interactions. In theory, an MS-based readout of deuterium label incorporation can overcome the concentration, size, purity, and complexity limitations inherent in NMR-based measurements of exchange; however, in practice, these advantages are reduced due to spectral interference and dilution of the sample in deuterium oxide (D_2O). In this study, we demonstrate that popular H/DX labeling strategies aggravate the interference problem and that significant recovery of spectral capacity may be achieved with a "minimalist" strategy. Simulations of peptide deuteration justify large reductions in the level of D_2O used in labeling experiments, as well as reduced numbers of peaks used in making relative labeling measurements between biochemical states of a protein. To demonstrate the utility of a minimalist approach, calmodulin was interrogated in a bottom-up H/DX-MS workflow, and sensitivity to the addition of Ca^{2+} as a structural perturbation was measured as a function of % D_2O and the number of peaks used in quantitating deuteration level. It is shown that high sensitivity to change is preserved with deuteration levels of 5.0 ± 1.1 (apo-CaM) and 1.4 ± 1.3% (holo-CaM) using 10% D_2O in the labeling experiment. Further, only two peaks of a peptide peak distribution are needed to sensitively monitor changes in protein structure, dynamics, or both.

Activities within the field of proteomics have grown to include high-throughput structural analyses. Although structural proteomics is typically the domain of X-ray crystallography and nuclear magnetic resonance (NMR) spectroscopy, methodologies involving MS and computational strategies have been under development particularly for the analysis of protein complexes. These include MS-based analyses of complexes transferred intact into the gas phase,[1] the identification of binding domains through cross-linking methods and bottom-up analysis of cross-linked peptides,[2] and a series of footprinting techniques, such as hydroxyl radical-mediated methods involving synchrotron radiation.[3] This latter technique has recently been used in conjunction with computational methods to support data-directed docking exercises.[4] Hydrogen/deuterium exchange (H/DX), however, is perhaps the most well-known method in this field.[5−7]

H/DX is a labeling technique that reports on protein structure, conformation, and ligation by monitoring changes in the exchange rate of labile hydrogens between the protein and D_2O. In general, amide hydrogens exhibit rapid exchange rates if they are accessible to the solvent and reduced exchange rates if they are hydrogen bonded, present in buried regions of a protein, or both.[6,8,9] Long the domain of NMR spectroscopy, H/DX with an MS-based detection system has an important role in the generation of data for protein folding,[10,11] conformational analysis,[12] ligand-induced structural perturbations,[13] and a series of approaches for the extraction of thermodynamic data on ligand binding.[14,15]

In applications involving the interrogation of multiprotein or protein−ligand interactions, it is typical to compare deuterium incorporation between two or more states, for example, ligand-bound and ligand-free. In this way, structural models of protein assemblies can be generated.[16,17] Localizing sites of altered exchange rates with higher resolution is usually conducted through a bottom-up strategy involving several steps: (i) preparation of protein interaction and control samples, (ii) deuterium exchange-in, (iii) quenching of exchange with low pH and temperature, (iv) proteolytic digestion with an acid-stable protease, and

* To whom correspondence should be addressed. Tel.: 403 210 3811. Fax: 403 270 0834. E-mail: dschriem@ucalgary.ca.

(1) Benesch, J. L. P.; Ruotolo, B. T.; Simmons, D. A.; Robinson, C. V. *Chem. Rev.* **2007**, *107*, 3544–3567.
(2) Vasilescu, J.; Figeys, D. *Curr. Opin. Biotechnol.* **2006**, *17*, 394–399.
(3) Xu, G. H.; Chance, M. R. *Chem. Rev.* **2007**, *107*, 3514–3543.
(4) Kamal, J. K. A.; Chance, M. R. *Protein Sci.* **2008**, *17*, 79–94.
(5) Tsutsui, Y.; Wintrode, P. L. *Curr. Med. Chem.* **2007**, *14*, 2344–2358.
(6) Wales, T. E.; Engen, J. R. *Mass Spectrom. Rev.* **2006**, *25*, 158–170.
(7) Engen, J. R.; Smith, D. L. *Anal. Chem.* **2001**, *73*, 256A–265A.
(8) Zhou, B.; Zhang, Z.-Y. *Methods* **2007**, *42*, 227–233.
(9) Mandell, J. G.; Falick, A. M.; Komives, E. A. *Anal. Chem.* **1998**, *70*, 3987–3995.
(10) Eyles, S. J.; Kaltashov, I. A. *Methods* **2004**, *34*, 88–99.
(11) Simmons, D. A.; Konermann, L. *Biochemistry* **2002**, *41*, 1906–1914.
(12) Englander, J. J.; Mar, C. D.; Li, W.; Englander, S. W.; Kim, J. S.; Stranz, D. D.; Hamuro, Y.; Woods, V. L. *Proc. Natl. Acad. Sci. U. S. A.* **2003**, *100*, 7057–7062.
(13) Hamuro, Y.; Coales, S. J.; Morrow, J. A.; Molnar, K. S.; Tuske, S. J.; Southern, M. R.; Griffin, P. R. *Protein Sci.* **2006**, *15*, 1883–1892.
(14) Tang, L.; Hopper, E. D.; Tong, Y.; Sadowsky, J. D.; Peterson, K. J.; Gellman, S. H.; Fitzgerald, M. C. *Anal. Chem.* **2007**, *79*, 5869–5877.
(15) Zhu, M. M.; Rempel, D. L.; Du, Z. H.; Gross, M. L. *J. Am. Chem. Soc.* **2003**, *125*, 5252–5253.
(16) Huzil, J. T.; Chik, J. K.; Slysz, G. W.; Freedman, H.; Tuszynski, J.; Taylor, R. E.; Sackett, D. L.; Schriemer, D. C. *J. Mol. Biol.* **2008**, *378*, 1016–1030.
(17) Mandell, J. G.; Falick, A. M.; Komives, E. A. *Proc. Natl. Acad. Sci. U. S. A.* **1998**, *95*, 14705–14710.

10.1021/ac800897q CCC: $40.75
Published on Web 08/16/2008

(v) LC−MS analysis (using electrospray or MALDI sources).[12,18,19] Automated systems for bottom-up strategies have been reported,[20] as has software for the extraction of deuterium levels.[21−23]

However, little progress has been made in optimizing the method for the analysis of low-abundance, complex protein mixtures. Such situations present analytical challenges related to speed of analysis, spectral interference, and sensitivity. As the chemical label in H/DX is transient even under quenched conditions,[24] bottom-up H/DX-MS analyses require completion in a short period of time relative to conventional proteomics exercises. The acid proteases used in H/DX-MS (e.g., pepsin) have low selectivity and generate large sets of peptides; these digests tend to have lower intensity than similar levels of the usual tryptic digests in proteomics, as basic amino acids are randomly distributed in the former. H/DX-MS experiments are routinely conducted with >90% D_2O for the exchange-in reaction.[6,25−33] This dilutes the protein sample, diminishes signal intensity, and broadens peptide peak distributions. Through the latter, spectral capacity is significantly reduced due to overlapping peak envelopes. Additionally, deuterium incorporation calculations proceed by subtracting the nondeuterated peptide average mass from the deuterated peptide average mass. It is conventional to use the entire distribution in these calculations, to obtain the average masses either through a simple centroiding function[23,34] or through a determination of a distribution of states.[22,35,36] In protein interaction applications where the sensitive detection of altered deuteration is sought, this approach may further reduce the spectral capacity of the system and negatively influence the precision of the measurement.

In this report, we explore alternative approaches to labeling and data extraction that can significantly improve the utility of the method for complex mixtures. We examined a range of labeling conditions and data extraction strategies, using a bottom-up H/DX-MS experimental approach applied to the protein calmodulin (CaM) in two different states: Ca^{2+}-free (apo) and Ca^{2+}-bound (holo). Specifically, the experiments involved the determination of relative deuterium incorporation levels between states using 10−75% D_2O in the labeling reactions and variable numbers of peaks selected from the full peak envelopes of the peptides generated in the workflow. The impact of these conditions on the precision of deuteration levels and the sensitivity of relative measurements of deuteration are assessed with the aid of simulations, and the implications for spectral capacity and sensitivity are discussed.

EXPERIMENTAL SECTION

Chemicals and Reagents. Trifluoroacetic acid (TFA), ethylenediaminetetraacetic acid (EDTA), sodium dihydrogen phosphate, potassium chloride, calcium chloride dihydrate, sodium hydroxide, D_2O (all >97% pure), and hydrochloric acid (37%) were purchased from Sigma-Aldrich (St. Louis, MO). Formic acid (FA, 98%) was acquired from Fluka (Buchs, Switzerland) while glycine (Gly, 99.7%) was obtained from GE Healthcare (Uppsala, Sweden). Immobilized pepsin (supplied as a slurry in 50% glycerol and 0.05 M sodium azide) was obtained from Pierce (Rockford, IL), and C_{18} particles (Magic 200 Å, 5 μm) were purchased from Michrom Bioresources (Auburn, CA). Ca^{2+}-free CaM (MW 16 707) was prepared and purified according to a previously established procedure[37] and provided by Dr. H. Vogel (Department of Biological Sciences, University of Calgary, Calgary, AB, Canada). Mobile phases were prepared using LC grade water and acetonitrile from Fisher Scientific (Fair Lawn, NJ).

Solutions. An aqueous, Ca^{2+}-free stock solution of CaM (356 μM) was prepared in 5 mM EDTA, aliquoted, and stored at −80 °C until use. The buffer solutions for the apo-CaM labeling experiments consisted of 100 mM KCl, 10 mM NaH_2PO_4, and 5 mM EDTA, pH 7.0. The holo-CaM buffer was the same with the exception of the addition of 2 mM $CaCl_2$ in place of EDTA. Chromatographic mobile phases consisted of 0.02% FA, 0.03% TFA, and 3% ACN (for mobile phase A) and 0.02% FA, 0.03% TFA, and 97% ACN (for mobile phase B). These solutions were vacuum degassed and sonicated prior to use.

Deuterium Labeling Conditions. Prior to conducting the deuterium exchange-in reaction, CaM stock solutions were diluted with an equal volume of 10× Ca^{2+} buffer (for holo-CaM) or 10× EDTA buffer (for apo-CaM), and this solution was 5-fold diluted with various ratios of H_2O/D_2O to ensure equivalent protein concentration (35 μM) and buffer composition for D_2O levels of 10, 25, 50, and 75% (v/v). Deuterium exchange-in was conducted for 2 min in a 20 °C water bath. The termination of labeling and the initiation of peptic digestion were achieved by adding an aliquot of the labeled sample (10 μL) to a chilled slurry of immobilized pepsin in 0.1 M Gly-HCl (pH 2.3). Digestion was performed under quench conditions on ice for 2.5 min with gentle mixing. Proteolytic digestion was terminated by centrifugation, and an aliquot of the chilled supernatant was immediately injected onto the LC−MS system for analysis. All analyses were performed in triplicate (from labeling to detection). In order to estimate the

(18) Hoofnagle, A. N.; Resing, K. A.; Ahn, N. G. *Annu. Rev. Biophys. Biomol. Struct.* **2003**, *32*, 1–25.
(19) Zhang, Z.; Smith, D. L. *Protein Sci.* **1993**, *2*, 522–531.
(20) Chalmers, M. J.; Busby, S. A.; Pascal, B. D.; He, Y.; Hendrickson, C. L.; Marshall, A. G.; Griffin, P. R. *Anal. Chem.* **2006**, *78*, 1005–1014.
(21) Pascal, B. D.; Chalmers, M. J.; Busby, S. A.; Mader, C. C.; Southern, M. R.; Tsinoremas, N. F.; Griffin, P. R. *BMC Bioinformatics* **2007**, *8*, 156–167.
(22) Hotchko, M.; Anand, G. S.; Komives, E. A.; Eyck, L. F. T. *Protein Sci.* **2006**, *15*, 583–601.
(23) Weis, D. D.; Engen, J. R.; Kass, I. J. *J. Am. Soc. Mass Spectrom.* **2006**, *17*, 1700–1703.
(24) Bai, Y.; Milne, J. S.; Mayne, L.; Englander, S. W. *Proteins Struct. Funct. Genet.* **1993**, *17*, 75–86.
(25) Wu, Y.; Kraveti, S.; Engen, J. R. *Anal. Chem.* **2006**, *78*, 1719–1723.
(26) Weis, D. D.; Wales, T. E.; Engen, J. R.; Hotchko, M.; Eyck, L. F. T. *J. Am. Soc. Mass. Spectrom.* **2006**, *17*, 1498–1509.
(27) Cravello, L.; Lascoux, D.; Forest, E. *Rapid Commun. Mass Spectrom.* **2003**, *17*, 2387–2393.
(28) Winters, M. S.; Spellman, D. S.; Lambris, J. D. *J. Immunol.* **2005**, *174*, 3469–3474.
(29) Wu, Y.; Engen, J. R.; Hobbins, W. B. *J. Am. Soc. Mass Spectrom.* **2005**, *17*, 163–167.
(30) Kipping, M.; Schierhorn, A. *J. Mass Spectrom.* **2003**, *38*, 271–276.
(31) Zhu, M. M.; Rempel, D. L.; Zhao, J.; Giblin, D. E.; Gross, M. L. *Biochemistry* **2003**, *42*, 15388–15397.
(32) Engen, J. R.; Gmeiner, W. H.; Smithgall, T. E.; Smith, D. L. *Biochemistry* **1999**, *38*, 8926–8935.
(33) Nemirovskiy, O.; Giblin, D. E.; Gross, M. L. *J. Am. Soc. Mass Spectrom.* **1999**, *10*, 711–718.
(34) Palmblad, M.; Buijs, J.; Håkansson, P. *J. Am. Soc. Mass. Spectrom.* **2001**, *12*, 1153–1162.
(35) Chik, J. K.; Graaf, J. L. V.; Schriemer, D. C. *Anal. Chem.* **2006**, *78*, 207–214.
(36) Abzalimov, R. R.; Kaltashov, I. A. *J. Am. Soc. Mass. Spectrom.* **2006**, *17*, 1543–1551.
(37) Matsuura, I.; Ishihara, K.; Nakai, Y.; Yazawa, M.; Toda, H.; Yagi, K. *J. Biochemistry* **1991**, *109*, 190–197.

degree of back-exchange observed throughout the experimental method, a 50 μM CaM solution (pH 7.0) was incubated for 72 h in 50% D_2O before proceeding with the analysis. Previous kinetic studies have indicated that full labeling has been achieved within this time frame (data not shown).

LC−MS System. The LC system consisted of a prototype low-flow isocratic pump and gradient pumps (Upchurch Scientific, Oak Harbor, WA), two Rheodyne six-port valves (Rohnert Park, CA), a 10-μL polyetheretherketone (PEEK) sample loop, and a C_{18} reversed-phase column (6.5 cm × 200 μm i.d., 5-μm particles). The C_{18} stationary phase was packed into the fused-silica capillary (Polymicro Technologies, Phoenix, AZ) in-house using a pressurized cell (Brechbühler Inc., Houston, TX). The injection valve, LC column, and fluid transfer lines were housed in an ice bath to minimize back-exchange of the deuterium label during analysis. Sample was loaded on column, washed with the isocratic pump (mobile phase A), and then separated using a linear gradient from 5 to 90% mobile phase B over 20 min. All chromatographic runs were performed at a flow rate of 4 μL/min. After each analysis, the column was regenerated with the starting mobile phase (5% mobile phase B), and the loading valve purged with injections of 50% ACN and 0.1 M Gly-HCl to minimize sample carryover between runs.

Peptide detection was achieved with a QSTAR Pulsar *i* quadrupole time-of-flight (QqTOF) mass spectrometer equipped with a turbo ion spray source and operated in TOF-MS mode (Applied Biosystems, Foster City, CA). Electrospray ionization was performed in the positive ion mode at 4.5 kV without nebulization gas, and data were collected in the m/z range of 300−1700. The data were then exported and processed for deuterium incorporation using software built in-house (see below).

Peptide Identification. Product ion mass spectra were collected on the QSTAR for unlabeled CaM digests prepared as above, using recursive information-dependent acquisitions until no additional peptides were detected. All resulting MS/MS spectra were searched against the CaM and pepsin sequences using an in-house installation of MASCOT (version 2.1).[38] Search terms included acetyl (N-terminal) and trimethyllysine as variable modifications, ±1.2 Da peptide mass tolerance, ±0.6 Da fragment mass tolerance, and 1+ to 3+ for peptide charge. All hits were manually verified. A final critera for acceptance was high-mass accuracy in an internally calibrated MS experiment (<50 ppm). Only peptides that were identified in this fashion were retained for deuteration measurement. A peptide data file containing the retention time, m/z, charge, peptide sequence, and start−stop number in the protein sequence for each peptide was then compiled. Altogether, 129 peptides were identified (100 nonredundant), which represents 96% of the CaM sequence.

Data Analysis. Software to automate deuterium incorporation calculations was developed using C# and Visual Studio.NET 3.0. As an input, the software requires a list of raw LC/MS.wiff files (generated from Analyst QSTAR instruments), a list of peptides (minimally consisting of m/z, retention time, and charge), and a configurable list of processing tasks. In one mode of analysis, the software generates extracted ion chromatograms (XIC) from peptide m/z values, performs chromatographic peak detection and selection, generates an averaged mass spectrum, and determines the intensities of the peaks within the corresponding peptide envelope. The centroid mass of the envelope is determined and deuteration level returned after subtraction of the centroid mass of the theoretical isotopic envelope of the peptide. The latter was incorporated from the.NET programming object "Molecular Weight Calculator" (version v3.1.2687) developed by Matthew Monroe at the Pacific Northwest National Laboratory (http://ncrr.pnl.gov/software). Additional processing tasks included Gaussian smoothing of the XIC and mass spectra. The software was further customized to allow the extraction of an array of deuterium incorporation values for each peptide, depending on the number of peaks included in the deuteration calculation.

With this software, deuterium incorporation for each peptide sequence was determined using 2−20 isotopes in the calculation. Isotopic profiles were manually validated to ensure correct chromatographic peak selection and to confirm the absence of spectral interference. To remove the effect of mass variance on centroid mass determinations, centroid mass measurements were made using the theoretical mass and the experimentally measured peak intensity (see Results and Discussion).

RESULTS AND DISCUSSION

In H/DX-MS, it is typical to establish experimental conditions where excess isotopic label is applied to maximize the population of exchangeable sites with label (approaching 100% incorporation), ostensibly to increase the sensitivity for detecting changes.[39] However, anything other than 100% deuterium incorporation increases the width of the isotopic distribution, increases the potential of spectral overlap, and decreases peak intensity. We sought to determine if precise quantitation of deuteration in H/DX-MS experiments (and in particular relative deuteration) can be achieved with low label incorporation and selective use of peaks within the distribution. Stable isotope tracer experiments in the field of environmental analysis very often quantitate tracer incorporation in a background isotopic distribution that contains a measureable amount of the tracer isotope itself.[40] In spite of this, precise quantitative measurements can be obtained even under conditions of extremely low tracer incorporation.[41] Thus, we argue that a similar approach could be effective in H/DX-MS studies.

To explore the relationship between isotope selection and labeling levels on the sensitivity of relative measurements of deuterium exchange, deuteration measurements were expressed in terms of Figure 1 and eqs 1−3. Peak-dependent deuteration levels are calculated as follows:

$$M_{\mathrm{av,T}} = M_{\mathrm{av}} + D_{\mathrm{av}} = M_0 + \frac{\sum_{i=1}^{n} ij_i}{\sum_{i=0}^{n} i} \qquad (1)$$

where $M_{\mathrm{av,T}}$ is the total average mass of the deuterated peptide, M_{av} is the mass of its natural isotopic distribution and D_{av} is the

(38) Perkins, D. N.; Pappin, D. J.; Creasy, D. M.; Cottrell, J. S. *Electrophoresis* **1999**, *20*, 3551–3567.

(39) Yan, X.; Deinzer, M. L.; Schimerlik, M. I.; Broderick, D.; Leid, M. E.; Dawson, M. I. *J. Am. Soc. Mass. Spectrom.* **2006**, *17*, 1510–1517.

(40) Meija, J.; Mester, Z. *Anal. Chim. Acta* **2008**, *607*, 115–125.

(41) Sturup, S.; Hansen, H. R.; Gammelgaard, B. *Anal. Bioanal. Chem.* **2008**, *390*, 541–554.

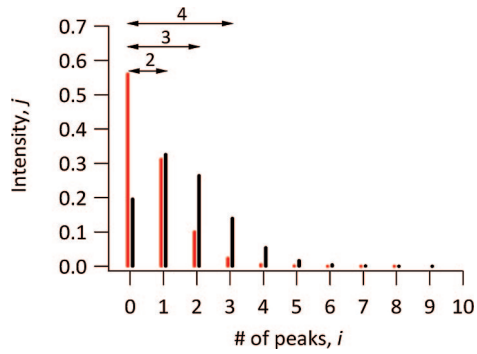

Figure 1. Theoretical isotopic distribution of a deuterated peptide (black) and nondeuterated peptide (red) referenced against the monoisotopic peak. The peptide illustrated is based on a sequence of averagine and a nominal mass of 1000 with 10 exchangeable sites. Arrows indicate examples of the number of peaks used in the measurement of deuteration level, beginning with the monoisotopic peak.

incremental mass arising from the distribution of deuterium induced by labeling. M_0 is the monoisotopic mass of the peptide, and the ratio of summations refers to the measurable intensities resulting from the convolution of the two distributions, expressed according to peak numbers i and their corresponding intensities j_i (Figure 1). A convenient rearrangement of eq 1 allows the determination of the average deuteration level for the peptide:

$$D_{av} = \frac{\sum_{i=1}^{n} ij_i}{\sum_{i=0}^{n} i} - (M_{av} - M_0) \tag{2}$$

Thus, the average deuterium level can be measured from the peak intensities corrected by the native isotopic distribution ($M_{av} - M_0$) for a given peptide. In relative labeling experiments, altered deuteration levels may be expressed as a ratio of two states (e.g., biochemically perturbed vs an unperturbed control),

$$D_R = \frac{D_{av,S}}{D_{av,C}} \tag{3}$$

Equation 2 was applied to a theoretical isotopic distribution of the calmodulin peptic peptide AELRHVMTNL expanded by various degrees of isotopic labeling (Figure 2A). Deuteration levels clearly increase with the % D_2O applied in the labeling experiment, and levels only reach a maximum when the entire distribution is used. This is supported by the actual labeling data for the peptide (Figure 2B). Further, the width of the distribution required to obtain maximum labeling levels increases with the degree of label incorporated. Extending the simulation to the measurement of deuteration ratios shows the impact of peak selection and labeling on the accuracy of ratio measurements (eq 3, Figure 3). Accuracy in ratio measurement also requires the selection of the full peak envelope, but large reductions in the degrees of labeling clearly provide an opportunity to minimize the expansion of the distribution.

If measurements of deuteration at low levels of deuterium incorporation are to be useful, the error in the measurement must be considerably lower in this regime, in order to preserve a sufficient signal-to-noise ratio (S/N). This is determined by the cumulative variability of peak intensities used in the calculation of deuteration. We modeled this variability in intensity to simulate the impact of peak noise on deuteration measurement sensitivity, to determine if a sufficient S/N would be preserved. These models are then compared to data obtained from an H/DX-MS study of apo- and holo-CaM. The noise regime experienced in the measurement of peak profiles by high-resolution MS can be sensitive to the intensities of the respective peaks in a distribution, as intensities can span the entire dynamic range of the instrument. We modeled noise to reflect this dependence on peak intensity and also considered the impact of background noise. In one model, peak noise is defined by a signal noise limit, with a minor contribution from detector noise at low signal levels. This may be expressed as in eq 4,

$$\sigma_{SL} = a\sqrt{(b + cx + dx^2)} \tag{4}$$

where σ_{SL} represents the standard deviation in the signal noise limit, and x the signal level ranging from 0 to 1 to represent the dynamic range of detection. Parameter a controls the severity of the noise overall, b the severity of detector noise, c adjusts the severity of the signal shot noise, and d the severity of the signal flicker noise.[42] In a second model, background noise is combined with signal noise and included simply as a fixed level normalized to the available dynamic range of the instrument (eq 5),

$$\sigma_T = \sqrt{\sigma_{SL}^2 + e} \tag{5}$$

where σ_T represents the total noise for the measured signal and e the parameter reflecting the severity of background noise.

As shown in eq 2, when isotopic resolution is available, mass values can be replaced with known peak numbers and the error in the measurement of D_{av} need only consider the contributions from the intensities j. Thus, the cumulative error in the deuteration level as a function of the number of peaks can be expressed through the relative standard deviation (RSD) in eq 6,

$$RSD_{av} = \frac{\sigma_{av}}{D_{av}} = \sqrt{\frac{\sum_{i=1}^{n} i\sigma(j_i)}{(\sum_{i=1}^{n} ij_i)^2} + \frac{\sum_{i=0}^{n} \sigma^2(j_i)}{(\sum_{i=0}^{n} j_i)^2}} \tag{6}$$

where RSD_{av} is the relative standard deviation of the deuteration level, and $\sigma(j_i)$ is the standard deviation of the peak intensity j at isotope i, drawn from the noise models above.

The standard deviation of the deuteration measurement, σ_{av}, derived from eq 6, is plotted as a function of the number of peaks used in the calculation assuming a model where signal flicker noise dominates ($d \ll c$, Figure 4A) and a model where signal shot noise dominates ($d \gg c$, Figure 4B), with 35% deuteration levels. This level was chosen for discussion as it represents the maximum average deuterium incorporation in our CaM data sets.

(42) Ingle, J. D.; Crouch, S. R. *Spectrochemical Analysis*; Prentice-Hall: Englewood Cliffs, NJ, 1988.

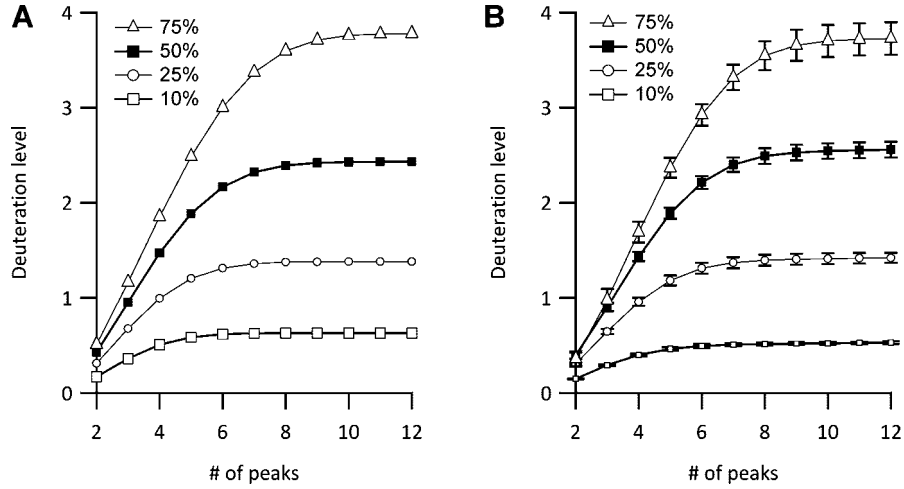

Figure 2. Influence of the number of peaks used in calculating the deuterium level, and % D_2O applied, on the measured deuteration level for peptide AELRHVMTNL based on (a) simulation of deuteration, assuming uniform back exchange of ~50% and (b) experimental data from a triplicate analysis of apo-CaM (error bars representing ± one SD).

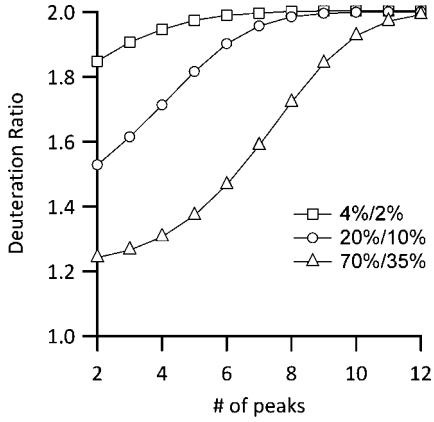

Figure 3. Simulation of the deuteration ratio D_r (eq 3), as a function of the number of peaks used in the calculation. The simulation is based on a peptide constructed of averagine (MW = 1000) with 10 exchangers and an expected deuteration ratio of 2 achieved using different absolute levels of D_2O applied.

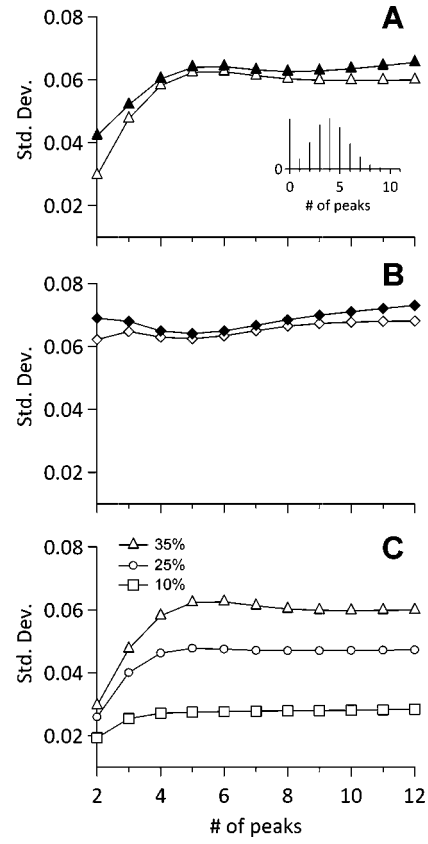

Figure 4. Effect of peak selection, beginning from the monoisotopic peak, on the standard deviation (σ_{av}) of deuteration measurements. (A) Simulation of peak noise assumes dominance of signal flicker noise ($d = 0.25$, $c = 0.0001$) for 35% deuteration of the peptide in Figure 2; inset shows peak distribution. (B) Simulation of peak noise assumes dominance of signal shot noise ($d = 0.0001$, $c = 0.05$) for the same peptide and % deuteration. (C) Effect of % deuteration on the standard deviation of deuteration, assuming noise characteristics of (A). (A) and (B) additionally show the effect of added background noise at a level of $e = 1 \times 10^{-6}$ (open symbols, signal noise; filled symbols, signal noise plus background noise).

Although labeling conditions were as high as 75% D_2O, back-exchange led to a retention of ~50% of the label incorporated, averaged over all peptides monitored. The impact of a model with random background noise added is also considered for both signal noise limits. Figure 4 demonstrates that the noise regime significantly impacts the precision in the deuteration measurement. Signals with low background noise in the signal flicker limit (Figure 4A, open triangles) will generate deuteration measurements where the precision is particularly sensitive to the number of peaks used in the measurement, but signals with low background in the signal shot limit (Figure 4B, open diamonds) are much less sensitive to the number of peaks used. In both cases, the inclusion of background noise levels deteriorates precision, particularly when low-intensity peaks on both extremes of the distribution are used in the calculation (see inset, Figure 4A). Assuming a signal flicker noise-dominated situation and varying only the degree of labeling, Figure 4C further shows that decreased deuteration improves precision in the deuteration measurement. Overall, these simulations demonstrate that error in deuteration measurements are at their lowest levels under conditions of reduced label incorporation, with the use of low numbers of peaks in the calculation. Based on error alone, this suggests that as few as two peaks may be used in precise

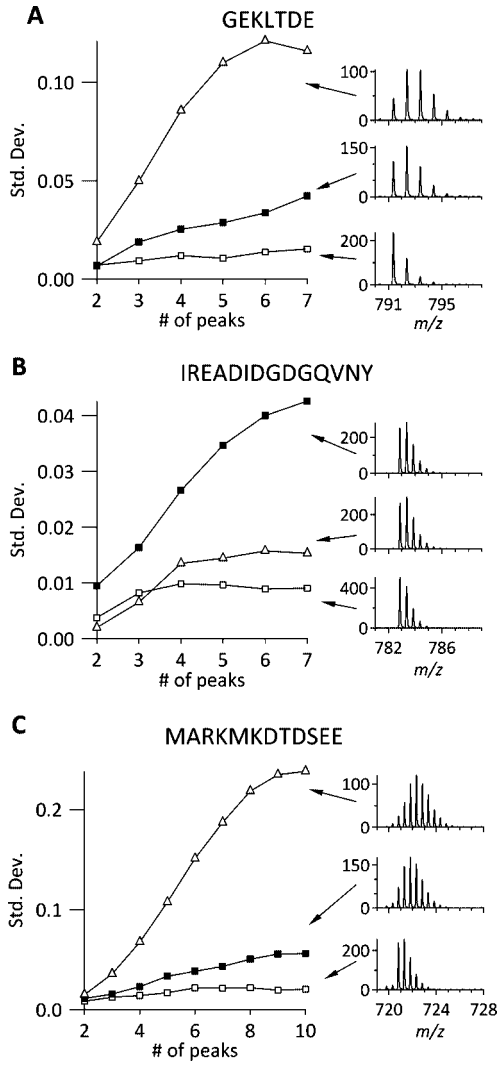

Figure 5. Three representative peptides from holo-CaM demonstrate the effect of increasing the number of peaks selected for deuteration calculation on the error in deuteration level measurements, for labeling experiments of 10 (open squares) 50 (filled squares), and 75% (open triangles). The insets indicate the corresponding peak profiles.

measurements of deuteration levels: the monoisotopic peak and the M + 1 peak.

To compare this with the data sets collected for CaM, we estimated the precision in deuteration measurements from triplicate analysis at several concentrations of applied label. Figure 5 shows three representative plots of standard deviation as a function of the number of peaks used in the deuteration measurement. These data confirm that maximum measurement precision is obtained at low label incorporation, and using the fewest number of peaks needed to estimate deuteration. Based on comparison with the simulations, the error curves correspond best to the signal flicker noise-limited model. This may be expected due to the relatively strong signals measured for CaM peptides in the QqTOF, but it may also suggest a contribution from the electrospray process itself as analyte flicker noise often arises from the sample presentation system.[42] Even though these data represent strong signals, the effect of background noise is apparent in certain cases (e.g., Figure 5A at 50% label applied), as evidenced by an increased slope at higher peak numbers where peak intensity is

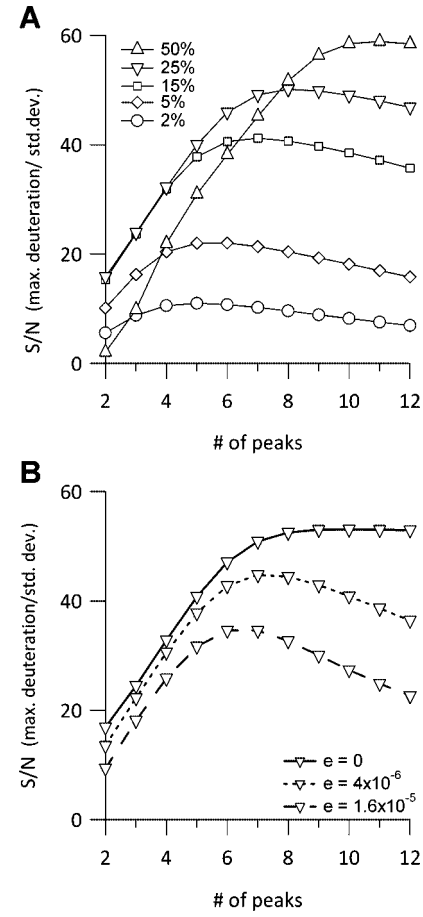

Figure 6. Simulation of the impact of peak selection on the sensitivity of deuteration measurements, expressed as the S/N ratio of the measurement, showing (A) the effect of % deuteration on sensitivity, assuming a noise model as in Figure 4A with background noise added, and (B) the effect of increasing background noise on sensitivity, assuming a fixed 25% deuteration level.

relatively low (cf. Figure 4A). Figure 5B presents an interesting anomaly in the deuteration of IREADIDGDGQVNY (residues 125−138) at the 75% labeling level. As the spectral insets show, this peptide clearly did not attain high levels of deuteration (only 2.8 ± 0.1%, compared to 2.2 ± 0.3% for 50% labeling and 0.23 ± 0.08% for 10% labeling, all for apo-CaM), suggesting that high concentration of D_2O influences the dynamics of calmodulin at least in this region of the structure. This is a concern for structural studies using H/DX and argues against the use of high D_2O concentrations. Such isotope effects have been documented in the field of protein structure and dynamics.[43,44]

Although the error is low under conditions of reduced deuteration and minimal peak selection, the sensitivity to changes in deuteration level is of greater importance in structural studies, as these changes highlight the impact of a structural perturbation such as the binding of a protein or small-molecule ligand. The sensitivity of the deuteration level measurement may be expressed as the RSD of the measurement as in eq 4, or its inverse the S/N. Figure 6A shows the simulation of the latter, displayed as a function of the number of peaks used in the calculation for several deuteration levels. Here, S/N is defined as the ratio of the deuteration level to the noise in its

(43) Cioni, P.; Strambini, G. B. *Biophys. J.* **2002**, *82*, 3246–3253.
(44) Panda, D.; Chakrabarti, G.; Hudson, J.; Pigg, K.; Miller, H. P.; Wilson, L.; Himes, R. H. *Biochemistry* **2000**, *39*, 5075–5081.

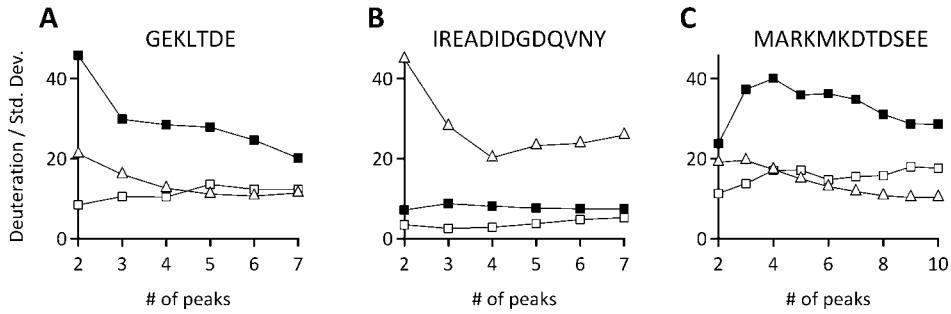

Figure 7. Sensitivity of the deuteration level measurement, expressed as the S/N ratio, for the three representative peptides from the holo-CaM data set shown in Figure 5. Sensitivity is shown as a function of the number of peaks selected for 10 (open square), 50 (filled square), and 75% (open triangle) labeling.

measurement. This plot shows that maximum sensitivity is achieved at high deuteration levels. However, although sensitivity is reduced at lower degrees of labeling, there is significant compensation seen as a result of lower noise. For example, comparing the maximums in Figure 6A, there is only a 2.4-fold difference in sensitivity between 50% deuteration and 5% deuteration. Further, labeling to 50% requires 10 peaks for maximum sensitivity and only 5 for 5%, suggesting a doubling of the spectral capacity for deuteration measurements in the lower labeling experiment. When spectral overlap is particularly severe, as would be expected in complex peptide mixtures, a two-pronged strategy involving reduced deuteration and peak selection restricted to a subset of the full envelope should preserve good sensitivity, which may exceed that of conventional conditions. In Figure 6B, the impact of background noise on sensitivity is evaluated in a similar fashion. It demonstrates that, with the inclusion of even low levels of background noise, there is a strong overall reduction in sensitivity. This figure further shows that attempts to select the full peak envelope in deuteration measurements can be misguided, as the low-intensity peaks at the extreme of the distribution only reduce sensitivity at a greater rate.

To compare these simulations with empirical data, Figure 7 displays the sensitivity in deuteration levels for a representative set of calmodulin peptides (see also Figure 5). Interestingly, almost all peptides exhibit maximum sensitivity below four peaks selected. In Figure 7A, the maximum sensitivity to change in deuteration level for GEKLTDE is found at two peaks for all label levels, and 50% labeling is more sensitive than 75% labeling (actual deuterium incorporation at 50% labeling is 15.5 ± 1.3%). Similar behavior is seen for the anomalous peptide IREADIDGDQVNY (Figure 7B), and although maximum sensitivity is at 75% labeling, actual deuterium incorporation is 2.8 ± 0.1%. In both cases, there is an apparent deviation from the simulations at the lower numbers of peaks used in the sensitivity measurement. This likely suggests a more complex noise model, but it is in part due to the short length of the peptide (Figure 7A) and very low label uptake (Figure 7B) shifting the maximum to lower peak numbers (simulations not shown).

Overall, it is clear that measurements involving the most intense and fewest number of peaks are required for highest sensitivity. When low label concentrations are used, this will almost always involve the monoisotopic ion and at most three successive peaks. This is emphasized by the sensitivity data for peptide MARKMKDTDSEE (Figure 7C). In the 50% labeling experiment, this peptide shows maximum sensitivity at four peaks, which encompasses the two most intense peaks in the distribution (peaks three and four; see Figure 5C). In the 75% labeling experiment, dilution and expansion of the isotopic envelope drops the signal levels to a noisier regime. Thus, low deuterium incorporation and the use of minimal numbers of peaks support sensitive measurements of altered deuteration, as suggested by the simulations. In all cases, selecting a number of peaks even lower than the native isotopic distribution of a peptide provides good sensitivity. While this may not correspond to the true deuteration ratio as suggested by Figure 3, in the detection of biochemically induced changes in labeling, accurate ratios are not required.[39]

These observations were tested on a wider analysis of the CaM data. The Ca^{2+}-saturated, holo form of CaM has a dumbell shape consisting of two globular domains connected by a long flexible "central helix" region encompassing residues 75−83.[45] As previous H/DX studies on the intact protein have shown, there is a substantial reduction in the population of fast-exchanging amides upon Ca^{2+} saturation, consistent with the adoption of a more compact, less solvent-accessible structure in these domains.[31,33] This is supported by circular dichroism measurements, where upon Ca^{2+} saturation, there is an increased degree of α-helicity in the total protein.[46] The minimalist approach to detecting the Ca^{2+}-induced perturbation via H/DX, as described in this study, should preserve the general structural conclusions of the previous structural work. Table 1 presents ratios of deuterium levels for Ca^{2+}-induced perturbation of CaM, for a representative set of peptic peptides representing 94% sequence coverage. Using the 75% labeling data with the full isotopic envelope as the standard, it is clear that changes in deuteration are broadly dispersed throughout the structure, with the exception of the flexible linker peptide between the two globular domains (e.g., MARKMKDTDSEEE, residues 74−84). This is expected, as saturating the two Ca^{2+}-binding "EF hands" in each domain generates significant conformational distortions in most regions of the domains but not in the linker.[45] In particular, all structural loops associated with Ca^{2+} complexation (represented by residues 16, 52−65, 88−102, and 125−138) are strongly reduced in labeling, as are all helices (encompassing residues 12−18, 13−18, 46−50, 49−54, 84−89, and 120−124) with the exception of the linker. This is consistent with a global tightening of all helices as described.[31,45] Aside from the domain linker, the loops between the Ca^{2+}-binding EF hands are the least affected by Ca^{2+}-binding

(45) Zhang, M.; Tanaka, T.; Ikura, M. *Nat. Struct. Biol.* **1995**, *2*, 758–767.
(46) Martin, S. R.; Bayley, P. M. *Biochem. J.* **1986**, *238*, 485–490.

Table 1. Deuterium Incorporation Ratios for Apo-/Holo-CaM Peptides for 10, 50, and 75% Labeling Conditions Calculated Using Either the Full Envelope or the Minimal Peak Method[a]

		75% labeling		50% labeling		10% labeling			
peptide sequence	residues	full	*P*-value	full	*P*-value	full	*P*-value	2 peaks	*P*-value
IREADIDGDGQVNY	125–138	0.08 (0.01)	0	0.09 (0.01)	0.0001	0.05 (0.02)	0.0001	0.07 (0.01)	0
EVDEM	120–124	0.12 (0.02)	0.0002	0.09 (0.01)	0	0	0.0031	0	0.0001
FKEAFSL	12–18	0.14 (0.04)	0.0006	0.09 (0.01)	0	0	0.001	0	0.0001
QDMINE	49–54	0.14 (0.05)	0.0011	0.15 (0.05)	0.001	0.12 (0.13)	0.0076	0	0.0015
AELQD	46–50	0.15 (0.02)	0.0001	0.11 (0.05)	0.0011	0.07 (0.04)	0.0006	0.13 (0.07)	0.0025
KEAFSL	13–18	0.16 (0.06)	0.0017	0.11 (0.00)	0	0	0.0002	0	0.0001
AFRVFDKDGNGYISA	88–102	0.17 (0.01)	0.0001	0.20 (0.02)	0.0002	0.22 (0.04)	0.0009	0.19 (0.02)	0.0003
EIREAF	84–89	0.17 (0.02)	0.0002	0.13 (0.01)	0	0.20 (0.01)	0	0.20 (0.01)	0.0001
INEVDADGNGTIDF	52–65	0.27 (0.02)	0.0003	0.30 (0.01)	0	0.35 (0.08)	0.0047	0.41 (0.04)	0.0013
AELRHVMTNL	103–112	0.32 (0.07)	0.0036	0.25 (0.01)	0.0001	0.20 (0.01)	0	0.31 (0.02)	0.0002
VQMMTAK	142–148	0.34 (0.02)	0.0004	0.30 (0.01)	0.0001	0.21 (0.06)	0.002	0.22 (0.03)	0.0004
FDKDGDGTITTKELGTVM	19–36	0.34 (0.03)	0.0008	0.35 (0.00)	0	0.34 (0.02)	0.0002	0.37 (0.05)	0.0017
RHVMTNL	106–112	0.43 (0.09)	0.0086	0.36 (0.01)	0.0002	0.28 (0.02)	0.0003	0.38 (0.04)	0.0017
IREAF	85–89	0.46 (0.32)	0.0003	0.11 (0.01)	0	0	0.0001	0	0.0001
RSLGQNPTEAEL	37–48	0.49 (0.04)	0.0022	0.45 (0.02)	0.0003	0.45 (0.06)	0.0034	0.51 (0.05)	0.0029
GEKLTDEE	113–120	0.58 (0.07)	0.0084	0.54 (0.05)	0.0041	0.43 (0.06)	0.0042	0.48 (0.08)	0.0088
ADQLTEEQIAE	1–11	0.63 (0.10)	0.025	0.55 (0.04)	0.0029	0.48 (0.03)	0.0011	0.59 (0.05)	0.0044
GEKLTDE	113–119	0.65 (0.06)	0.0101	0.58 (0.05)	0.0046	0.52 (0.07)	0.0068	0.51 (0.08)	0.0089
MARKMKDTDSEEE	*72–84*	*0.82 (0.09)*	*0.0675*	*0.75 (0.05)*	*0.0115*	*0.78 (0.08)*	*0.0386*	*0.79 (0.08)*	*0.045*
MARKMKDTDSEE	*72–83*	*0.84 (0.10)*	*0.1161*	*0.77 (0.06)*	*0.019*	*0.77 (0.07)*	*0.0294*	*0.76 (0.10)*	*0.0574*

[a] Data are reported as D_{holo}/D_{apo} (standard deviation in parentheses) with statistical signifance indicated by *p*-values and sorted according to diminishing relative deuteration at 75% labeling (ratio approaching 1). Domain linker peptides are highlighted in italics.

(peptides 37−48 and 113−119), which is further supported by an analysis of NMR and X-ray crystal structures for the apo/holo forms of CaM.

These results are paralleled in the data obtained from 50% labeling down to 10% labeling using as few as two peaks (monoisotopic and the M + 1 peaks, Table 1). As a comparison of the ratios between these sets and the set represented by 75% show, the ordering of the ratios is preserved with few exceptions. For example, even though the Ca^{2+}-induced change in labeling for MARKMKDTDSEEE is low in 75% labeling (ratio of 0.82 ± 0.09), a similar ratio is measured for 10% labeling and two peaks (0.79 ± 0.08). All large changes in deuteration are readily detected with a minimalist approach, although at 10% labeling and two peaks, entries of zero in the ratio columns indicate no measurable deuteration in the holo-CaM analysis. The most obvious difference between 75% labeling and 10% labeling experiments is found for peptide IREAF (residues 85−89). The former reports this region of CaM as undergoing a small but significant change in deuteration, whereas the latter reports a large and significant change. This does not appear to be due to reduced sensitivity under low-labeling conditions, as the 50% labeling data agree more closely to the 10% data, but may simply be due to the low precision of the measurement at 75% labeling. Overall, Table 1 demonstrates that a minimalist approach offers a discriminating power similar to the conventional strategy, even though at 10% D_2O in the labeling reaction, average deuterium incorporation across all peptides is only 5.0 ± 1.1% for apo-CaM and 1.4 ± 1.3% for holo-CaM.

CONCLUSIONS AND SIGNIFICANCE

This study demonstrates that robust measurements of structural perturbations via H/DX-MS can be preserved through a minimalist strategy involving substantially lower concentrations of D_2O in forward exchange measurements and that measurements using as few as the monoisotopic peak plus one afford opportunities to significantly increase spectral capacity. As suggested above, reduced D_2O concentrations have the added advantage of minimizing sample dilution and preserving peak intensities through reduced expansion of the isotopic envelope, which will support the use of H/DX experiments in situations where only small amounts of protein are available (e.g., endogenous levels). Further, as seen in the treatment of calmodulin with 75% D_2O, high label concentrations can distort the native structure/dynamics of the protein, arguing that such concentrations should be avoided if possible.

The retention of high S/N in deuteration measurements should have value beyond the differential measurements discussed in this study, in studies of protein folding by H/DX, for example. However, there may be limitations encountered in differentiating EX1 from EX2 kinetics of exchange, arguing for the use of the full isotopic envelope and possibly higher levels of D_2O. This has not been tested in the current work, but a recent study suggests that the detection of mixed states need not require the full resolution of overlapping envelopes.[35] Of greater concern, the degree of deuterium uptake will vary across a range within the peptides of a given protein. Thus, one given labeling condition may "overlabel" a peptide with a high deuteration rate but "underlabel" one with a low deuteration rate. While we have demonstrated that the S/N range accessible with reduced labeling accommodates ratio measurements for calmodulin-derived peptides, it is possible that larger protein systems may require additional D_2O levels for a given incubation time, to ensure the greatest discrimination across the full peptide set is achieved.

Overall, the advantages of this approach provide a basis for extending H/DX-MS methods to the analysis of significantly larger protein complexes and provide an opportunity for improvements in automated data collection. While the data described in this study were not challenged with high spectral interference or high background noise levels, such situations could easily occur in more complex systems and will be explored in future studies.

ACKNOWLEDGMENT

G.W.S. and A.J.P. contributed equally to the manuscript.

Received for review May 1, 2008. Accepted July 17, 2008.

AC800897Q